Cirrus and water vapor in the tropical tropopause layer observed by Upper Atmosphere Research Satellite (UARS)

Cirrus and water vapor in the tropical tropopause layer observed by Upper Atmosphere Research Satellite (UARS)

H. L. Clark
Centre National de Recherches Météorologiques, Toulouse, France

R. S. Harwood, A. Billingham, and H. C. Pumphrey
School of GeoSciences, University of Edinburgh, Edinburgh, UK

Received 6 May 2003; revised 8 September 2003; accepted 15 September 2003; published 17 December 2003.

[1] The Microwave Limb Sounder (MLS) on Upper Atmosphere Research Satellite (UARS) is sensitive to water vapor and ozone in the lower stratosphere. The Cryogenic Limb Array Etalon Spectrometer (CLAES), another of the instruments on UARS, has a spatial and temporal coverage similar to that of MLS and can be used to indicate the presence of cirrus. We examine the relationships among water vapor, ozone, and cirrus in the tropical region at 68 and 83 hPa during December–February 1991/1992, an El Niño period. For most longitudes at 68 hPa, three-dimensional trajectories show that the cirrus form predominately in air which ascends slowly through the tropical tropopause layer. Cirrus form in air which has travelled a long way in the horizontal, in the westerly jet, before heading equatorward in subtropical anticyclones. In the Indonesian region, however, a greater proportion is found in air which is sinking than in air which is ascending. The western Pacific region sees the highest proportion of cirrus which may have been influenced by convection, and the possible contribution from convection is greater at 83 hPa than at 68 hPa. In cloudy regions, the air is likely to have a high relative humidity. Mixing ratios of ozone from MLS have a tendency to be lower, and this may indicate that ozone is destroyed on the ice particles that comprise the clouds. *INDEX TERMS:* 0341 Atmospheric Composition and Structure: Middle atmosphere—constituent transport and chemistry (3334); 3334 Meteorology and Atmospheric Dynamics: Middle atmosphere dynamics (0341, 0342); 3362 Meteorology and Atmospheric Dynamics: Stratosphere/troposphere interactions; 3360 Meteorology and Atmospheric Dynamics: Remote sensing; *KEYWORDS:* stratosphere/troposphere exchange, subvisible cirrus, water vapor

Citation: Clark, H. L., R. S. Harwood, A. Billingham, and H. C. Pumphrey, Cirrus and water vapor in the tropical tropopause layer observed by Upper Atmosphere Research Satellite (UARS), *J. Geophys. Res.*, *108*(D24), 4751, doi:10.1029/2003JD003748, 2003.

1. Introduction

[2] Explaining the dryness of the lower stratosphere is a longstanding issue. *Brewer* [1949] proposed that air entering the stratosphere from the troposphere in the tropics is "freeze dried" by the cold and high tropical tropopause or "cold trap", but exactly how and where this dehydration takes place is still unclear. Sometime during its ascent from a level near the top of deep convection (around 150 hPa) to a level of about 50 hPa, air becomes dehydrated to mixing ratios characteristic of the stratosphere. This transition zone is often known as the tropical tropopause layer [*Sherwood and Dessler*, 2000; *Gettelman and de Forster*, 2002].

[3] Large-scale ascent and mass transfer through the tropical tropopause layer takes place under the action of the extratropical pump [e.g., *Eliassen*, 1951; *Dickenson*, 1968] which drives an annual cycle in tropical temperatures near the 100 hPa level due to hemispheric and seasonal asymmetry of the planetary waves. The lowest temperatures occur during northern winter and highest temperatures during northern summer. Consequently, mixing ratios of air entering the stratosphere from the tropical troposphere have also an annual cycle, in phase with the tropopause temperatures [*Mote et al.*, 1995, 1996].

[4] There are some problems with this zonal mean view. Firstly, the lowest mean tropopause temperatures are not low enough to explain the lowest mean mixing ratios in the stratosphere [*Mote et al.*, 1996]. Some recent satellite and aircraft data [*Michelsen et al.*, 2000; *Zhou et al.*, 2001] also showed this. It is often envisaged therefore, that the air enters the stratosphere in preferred locations such as over the "stratospheric fountain" region as defined by *Newell and Gould-Stewart* [1981]. More recently, *Dessler* [1998] reexamined the stratospheric fountain hypothesis and found that the volume mixing ratio of water vapor entering the stratosphere agreed well with the saturation volume mixing ratio of the tropical tropopause region and therefore that the stratospheric fountain hypothesis was unnecessary. There remains some debate over this issue [*Vömel and Oltmans*, 1999; *Dessler*, 1999]. The stratospheric fountain idea was also questioned by *Sherwood* [2000] and *Gettelman et al.*

0148-0227/03/2003JD003748

[2000], who found evidence for sinking motion in the fountain region, prompting *Holton and Gettelman* [2001] to investigate the importance of horizontal transport through the fountain or cold trap.

[5] Secondly, uniform rising motion across the tropics might be expected to result in a layer of cirrus clouds forming near the tropopause. Since this cirrus layer had not been observed, it was suggested [e.g., *Robinson*, 1980] that upward flow across the tropopause must be associated with deep convection that penetrates the stratosphere. Tropical convective systems could dry the stratosphere through mechanisms such as that proposed by *Danielsen* [1982] or by *Potter and Holton* [1995]. *Danielsen* [1982] suggested that convective events might be strong enough to overshoot the tropopause, mixing tropospheric air with stratospheric air and leading to the formation of a large cirrus anvil in the stratosphere. *Potter and Holton* [1995] suggested that convectively generated buoyancy waves could also induce vertical parcel displacements which promote the formation of ice crystals in the lower stratosphere. Potter and Holton's mechanism, like Danielsen's, results in dehydration but does not require convection to penetrate the tropopause or reach the hygropause.

[6] Satellite observations [*Wang et al.*, 1996; *Mergenthaler et al.*, 1999] have shown that cirrus is in fact distributed more widely than originally thought. These observations are primarily of subvisible cirrus, so named because they cannot be seen from the ground. Their optical depth falls in the range $0.0002 < \tau < 0.03$ [*Sassen and Cho*, 1992]. The formation of these subvisible cirrus is not entirely understood. They may form as a result of overshooting convection or as the result of slow, wave-driven ascent. Cirrus clouds can have a strong radiative effect [*Liou*, 1986; *Ramanathan and Collins*, 1991; *Jensen et al.*, 1999] and radiative heating rate near the tropical tropopause is critical for determining the water balance of the stratosphere. *Jensen et al.* [1996] showed that subvisible cirrus near the tropopause can govern the water vapor input into the lower stratosphere by simultaneously removing water vapor by sedimentation and lofting the air through IR heating. *Hartmann et al.* [2001] showed that tropopause cirrus crucially affects the heat balance of the stratosphere and may be important in dehydrating the air. Thus the study of thin cirrus may contribute to our understanding of the dehydration, dynamics, and radiative balance of the tropical tropopause layer.

[7] In this paper, we investigate the dynamical and chemical environment of subvisible cirrus near the upper limit of the tropical tropopause layer to see if their observation can give any indications of the relative importance of the different mechanisms of stratosphere-troposphere exchange. We use trajectory analysis to distinguish between uniform or local ascent. In section 2 we describe the data used. Section 3.1 examines the vertical motion of the air in which the cirrus clouds have formed, and section 3.2 describes their chemical environment. Conclusions are presented in section 4.

2. Data

[8] Upper Atmosphere Research Satellite (UARS) [*Reber*, 1993] is in an almost circular orbit at an altitude of 585 km and an inclination of 57° to the equator. It makes about 15 orbits a day. The Microwave Limb Sounder (MLS) and the Cryogenic Limb Array Etalon Spectrometer (CLAES) are both limb viewing instruments mounted on UARS. The MLS instrument is described in more detail by *Barath et al.* [1993] and the measurement technique by *Waters* [1993]. A description of the CLAES instrument is given by *Roche et al.* [1993]. MLS and CLAES have similar viewing characteristics, their footprints being separated by less than 30 s and less than 200 km along the measurement track at all times [*Read et al.*, 2001]. Their daily coverage extends from between 80°N and 34°S switching to 34°N and 80°S about every 36 days due to the satellite making a yaw manoevre. The tropical region is thus, barring occasional instrument problems, observed daily.

[9] From MLS we make use of water vapor and ozone measurements in the lower stratosphere. We use version 104 measurements of water vapor from the 183 GHz radiometer which cover the period 19 September 1991 to 22 April 1993. Version 104 is not the most recently released version, version 5, but provides some advantages over it. A full description of the version 104 lower stratospheric water vapor product is given by [*Pumphrey*, 1999], and some of its advantages over version 5 are discussed by *Pumphrey et al.* [2000]. In the most part, we confine our study to the 68 hPa level where we have most confidence in the MLS water vapor product. We estimate at this level, the precision of a single profile to be 0.3 ppmv and the accuracy to be 0.75 ppmv. The ozone data come from the 205 GHz radiometer on MLS and we use the most current version, version 5. The validation of the ozone measurements is given by *Froidevaux et al.* [1996], and a description of the version 5 ozone data is given by *Livesey et al.* [2003]. At 68 hPa the precision of a single profile is estimated to be 0.25 ppmv and the accuracy to be about 0.4 ppmv.

[10] From CLAES, we use version 9 extinction coefficients from the 780 cm^{-1} aerosol channel and follow the method of *Mergenthaler et al.* [1999] to identify the presence of high clouds and filter out any possible contamination by Mount Pinatubo aerosol. The clouds are detectable against the background aerosol because they are more opaque in the infrared. *Mergenthaler et al.* [1999] used a cloud threshold filter on version 8 data which was set at a level such that the background aerosol signal was excluded. We use the same threshold for version 9 data which excludes more cases which could be Pinatubo aerosol.

[11] CLAES made scientific measurements over the period 1 October 1991 to 5 May 1993, when the cryogens evaporated and the instrument warmed up. This period overlaps with the operational period of the 183 GHz radiometer of MLS. MLS is relatively insensitive to the occurrence of cirrus clouds. On the basis of expected scattering properties for radiation at 183GHz of the likely cloud ice content and effective particle sizes as reported by *Mergenthaler et al.* [1999], M. J. Filipiak (personal communication 2003) estimates that the effects of the clouds on the water vapor retrievals are less than 2%.

[12] We also make use of various data from the European Centre for Medium Range Weather Forecast's (ECMWF) Reanalysis data (ERA-15) [*Gibson et al.*, 1997], and outgoing longwave radiation (OLR) from the Advanced Very High Resolution Radiometer (AVHRR) [*Liebmann and*

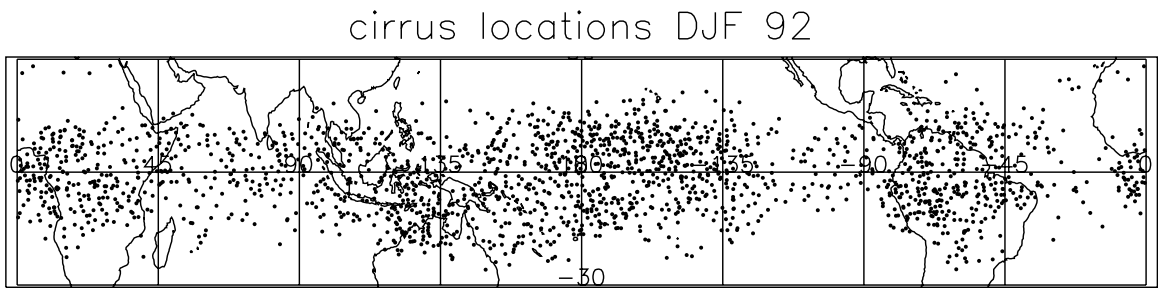

Figure 1. Seasonal average of CLAES cirrus cloud observations.

Smith, 1996]. Both these data sets are available on a 2.5° by 2.5°E grid.

3. Cirrus and Their Environment

[13] Subvisible cirrus in the upper region of the tropical tropopause layer have been noted from satellite data and from in situ observations. Lidar measurements from a 10 day space shuttle mission in September 1994 [*Winker and Trepte*, 1998] revealed cirrus at 17 km and Lidar measurements from an aircraft mission during December 1995 and February 1996 [*Pfister et al.*, 2001] revealed cirrus at altitudes exceeding 18 km. The Stratospheric Aerosol and Gas Experiment (SAGE) II and CLAES, both show that cirrus are found up to altitudes of 18.5 km [*Kent et al.*, 1995; *Wang et al.*, 1996; *Mergenthaler et al.*, 1999]. Seasonal climatologies show that subvisible cirrus occur over much of the tropics but preferentially in the convectively active regions over the continental landmasses and the western Pacific ocean. See *Wang et al.* [1996] and *Mergenthaler et al.* [1999] for figures showing the seasonal frequency of occurrence of cirrus at altitudes in the tropical tropopause layer.

[14] Figure 1 shows the locations of CLAES cloudy footprints at 68 hPa collected throughout the December–February (DJF) period of 1991/1992. The highest densities of cirrus are located over the more convectively active regions of the central and western Pacific and over South America and equatorial Africa. The year 1992 was an El Niño year, which may explain the concentration of cirrus clouds centered nearer to the dateline [*Massie et al.*, 2000], farther eastward than might be expected under normal conditions. *Wang et al.* [1996] and *Kent et al.* [1995] found that the frequency of cirrus formation in the tropics increased during the El Niño of 1987 at altitudes of 13–15.5 km, whereas *Mergenthaler et al.* [1999] showed that the frequency of cirrus formation at about 18 km was less in the El Niño period of DJF 1991/1992 than during the same season of the following year. They suggested that this interannual difference may be partly attributable to the affects of Pinatubo aerosol which may have reduced the penetration of solar radiation to the tropics in 1991/1992 resulting in less convective activity reaching to high levels. *Luo et al.* [2002] found that Mount Pinatubo aerosol did not have a widespread systematic effect on the amount of tropical cirrus although a local influence may be still be apparent. The effects of volcanic eruptions and El Niño and the interplay between the two remain uncertain.

3.1. Trajectory Analysis

[15] In order to discover more about the origins of the cirrus clouds in the tropical tropopause region, we perform a three-dimensional trajectory analysis. The trajectory model is described by *Methven* [1997]. It uses three-dimensional gridded winds from the ECMWF analyses which are interpolated to the trajectory locations using bilinear interpolation in the horizontal and in time, and cubic Lagrange interpolation in the vertical. Advection is performed with a fourth-order Runge-Kutta scheme and a 0.6-hour step size [*Jackson et al.*, 2001]. The reanalysis fields are updated every 6 hours. We have found that sampling less frequently than every 6 hours leads to systematic errors because of a poorly sampled diurnal cycle of convection.

[16] We initialize trajectories at each of the cirrus cloud locations shown in Figure 1 during the DJF 1991/1992

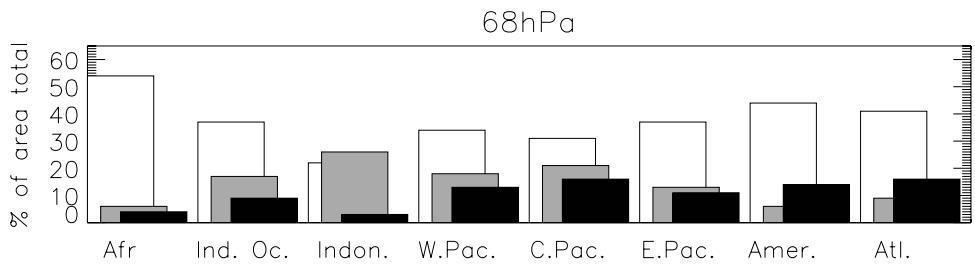

Figure 2. Percentage number of cirrus in each longitude sector at 68 hPa which were formed in air having undergone (1) ascent at a rate comparable to the zonal ascent rate (white), (2) air that has descended (black), and (3) air that has rapidly ascended (grey). The total number of trajectories in each 45° longitude sector are as follows: Africa, 246; Indian Ocean, 145; Indonesia, 221; western Pacific, 300; central Pacific, 394; eastern Pacific, 127; the Americas, 311; and Atlantic, 113.

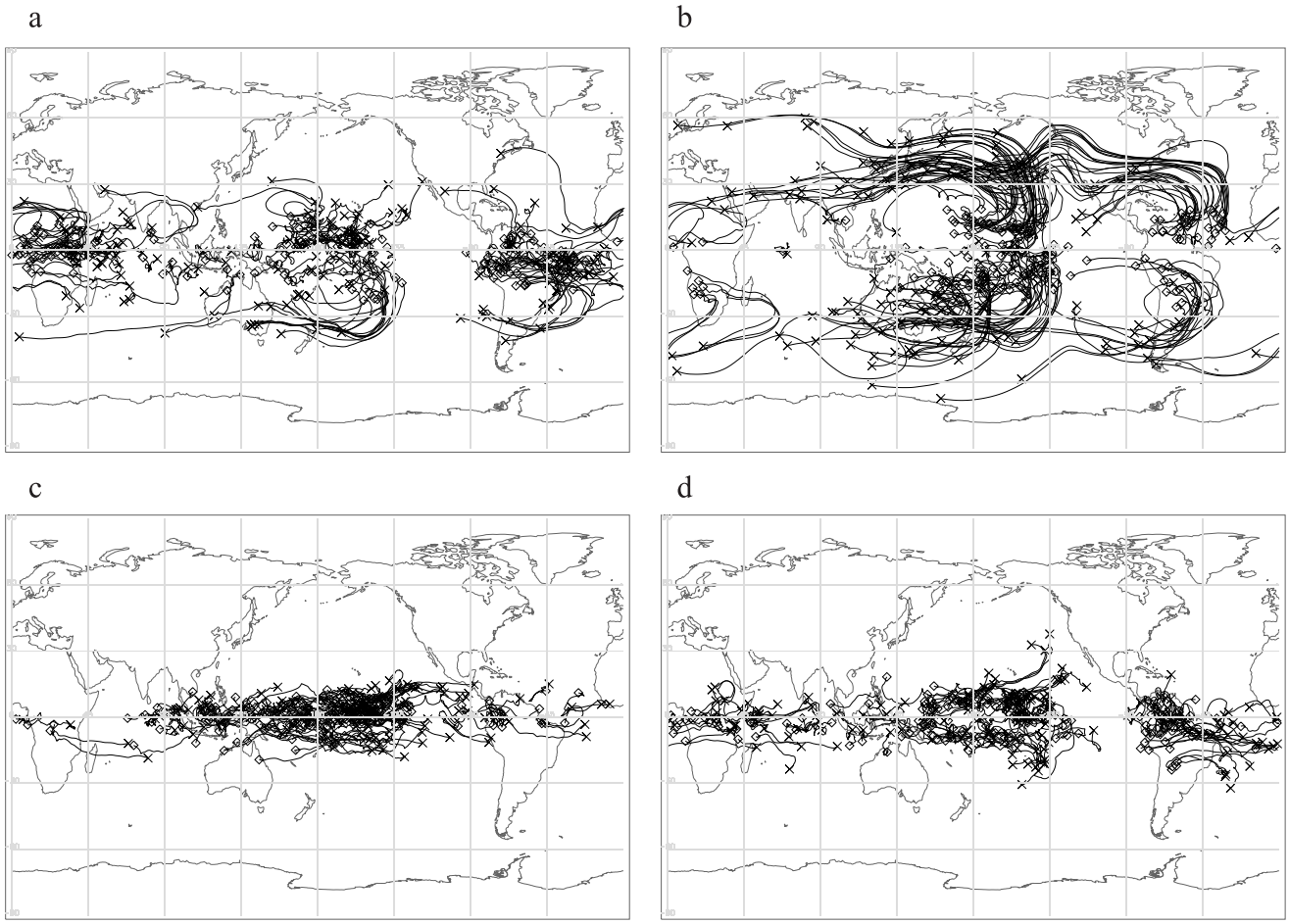

Figure 3. Samples of trajectories for each category of vertical motion. (a) Trajectories which have ascended at the rate of the zonal mean uplift, (b) trajectories which have ascended 10 times more quickly than the zonal ascent rate, (c) trajectories which have descended, and (d) trajectories which have experienced little vertical motion. Crosses mark the starting position of a 10-day trajectory which ends on a cirrus observation at 68 hPa (diamonds).

period and the trajectories are run backward in time for 10 days. There are 1857 trajectories in total for this time period. We initialize the trajectories on the 68 hPa level, the level at which CLAES data are reported for the standard level 3 AT output. The 68 hPa surface is centered near 19 km but since the CLAES instrument has a vertical resolution of about 2.5 km a cloud reported at 19km may be found nearer to 17 km [*Mergenthaler et al.*, 1999]. We therefore also initialize trajectories at 83 hPa, to give an indication of how different the results would be if all the CLAES clouds were to fall near this lower level.

[17] The trajectories are classified according to the vertical motion to which they have been subjected. We divide the 30°N–30°S region into 45° longitude bands and count the number of trajectories in each bin which have either (1) undergone a vertical ascent at a rate comparable to the zonal ascent rate, approximately 0.3 mm s^{-1} [e.g., *Mote et al.*, 1996], (2) ascended at a rate greater than 2 km over 5 days [e.g., *Gettelman et al.*, 2002] roughly equivalent to an order of magnitude greater than the zonal mean ascent rate, (3) descended, or (4) have remained close to the 68 hPa surface. The results are shown in Figure 2. It must be remembered that these trajectories have also traveled several hundred kilometers in the horizontal over the 10 day trajectory period as discussed further below.

3.1.1. Trajectories Ending at 68 hPa

[18] Figure 2 shows that for all sectors except for Indonesia, the highest contribution to the cirrus at 68 hPa comes from trajectories that have undergone ascent at a rate comparable to the zonal-mean ascent rate. In the African region, this contributes to about 55% of the cirrus and to about 40% in most of the other sectors. Figure 3a shows a representative sample of 150 of the trajectories which fell into this "slow ascent" category. Trajectories begin on the crosses and end on the diamonds where the cirrus observation by CLAES was made. It is seen that these trajectories originate primarily within the 30°N–30°S region and travel equatorward in the subtropical anticyclones over the western Pacific. Similar anticyclonic motion can be seen over Africa and South America.

[19] A small proportion of cirrus, around 15% in the central and western Pacific, are formed in air parcels which have experienced an ascent rate which is too fast to be explained by the zonal ascent rate of the Brewer-Dobson circulation. The trajectory history of these parcels, plotted in Figure 3b, reveals that many have been advected toward the

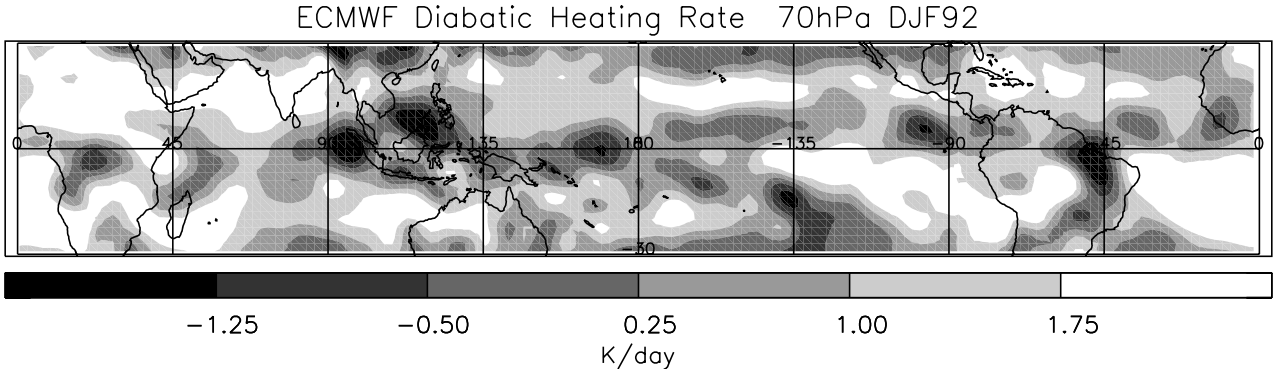

Figure 4. Seasonal average of ECMWF diabatic heating rate at 70 hPa.

equator from well outside the tropical region and have travelled a long way in the horizontal. They have often originated in midlatitudes and moved swiftly in the westerly jet before being advected toward the equator in an anticyclonic fashion. This anticyclonic pattern to the trajectories is similar to that for the slow ascent trajectories discussed above but encompasses a wider latitudinal spread.

[20] Cirrus associated with upper tropospheric or lower stratospheric anticyclonic flow have been widely observed by in situ measurement campaigns and can be the result of cyclone-scale uplift, overshooting convective cloud turrets embedded in the cyclonic systems, and cyclone-generated gravity waves. The Stratosphere-Troposphere Exchange Project (STEP-tropical) [*Danielsen*, 1993] showed that anticyclonic motion associated with the Australian monsoon system mixed tropospheric air into the stratosphere leading to widespread "umbrella" shaped layers of cirrus at around 18 km. Smaller-scale overshooting cloud turrets were also observed which were related to continental maritime air and left anvil shaped cirrus clouds in the stratosphere. Associated gravity waves [*Pfister et al.*, 2001] may also make a contribution to the "rapid ascent" cirrus. *Pfister et al.* [2001] ran back trajectories from cirrus observed at 18 km by an aircraft-based lidar during the Tropical Ozone Transport Experiment/Vortex Ozone Transport Experiment (TOTE/VOTE) in December 1995 and February 1996. They observed many air parcels to be advected eastward in the subtropical jet before drifting equatorward in the central Pacific region. The air parcels then return westward in the easterly flow along the equator and may, if sufficiently close to the cold point tropopause, be dehydrated in the cold trap region as suggested by *Holton and Gettelman* [2001]. Similarly, our trajectories show that air parcels traveled a long way in the horizontal. The cirrus here however, are found near the upper boundary of the TTL and while they are probably above the cold point tropopause, that might not be the coldest temperature encountered by the trajectory on its quasi-horizontal route. Thus the dehydration associated with the cirrus at this altitude may not be the only or principal dehydration process.

[21] In the Indonesian, western Pacific and central Pacific sectors, Figure 2 shows that there is a substantial proportion of cirrus associated with trajectories that have descended. In the Indonesian region (90–135°E) the contribution from descent outweighs that from ascent. The results are in support of *Sherwood* [2000] and *Gettelman et al.* [2000], who questioned the idea of the stratospheric fountain and showed results which suggested that air is descending. Following *Norton* [2001], we have calculated the ECMWF diabatic heating field for DJF 1992 at 70 hPa (Figure 4) to illustrate geographically where the descending motion is taking place. The diabatic heating field is smoother than the vertical velocity field used in the trajectory calculations but broadly consistent with it. Figure 4 shows that regions of cooling or weak heating, where the cirrus are associated with descending air, are found primarily over Indonesia, the western Pacific and above the ITCZ in the central Pacific sector. *Norton* [2001] plotted the 1980–1996 DJF seasonal average diabatic heating fields for 70 hPa and 268 hPa along with AVHRR OLR, and noted an almost inverse circulation in the lower stratosphere to that in the upper troposphere, with descending air near the top of the tropical tropopause layer being found over convective regions.

[22] The formation of these cirrus in air which is apparently sinking and cooling is perhaps surprising. Some might be formed in the cold regions of downward propagating Kelvin waves generated by deep convection [*Boehm and Verlinde*, 2000] or explained by the model of *Hartmann et al.* [2001] and *Holton and Gettelman* [2001]. They showed that when cirrus lie directly above deep convection, radiative cooling and subsidence can result. Horizontal advection of moist air can provide the moisture source to maintain the thin cirrus and subsequent particle sedimentation would lead to dehydration. Figure 5 shows the seasonally averaged OLR with low values indicating where deep convection is taking place. As *Norton* [2001] found, there is a correspondence between the OLR (Figure 5) and the diabatic heating field (Figure 4). The areas of cooling or weak heating where we have observed the cirrus to be located, do generally lie above areas of deep convection thus offering some evidence in support of the mechanism of *Hartmann et al.* [2001] and *Holton and Gettelman* [2001].

[23] The three categories of vertical motion (zonal ascent, descent and rapid ascent) account for about 70% of the cirrus trajectories. The fourth bin accounts for those which have remained close to the 68 hPa surface and have experienced very little vertical motion. These trajectories originate within 15°N and 15°S as can be seen in Figure 3d in the slower moving air between the two subtropical anticyclones. They have travelled on average, a shorter distance than those trajectories which have ascended at either the zonal mean ascent rate, or 10 times more rapidly.

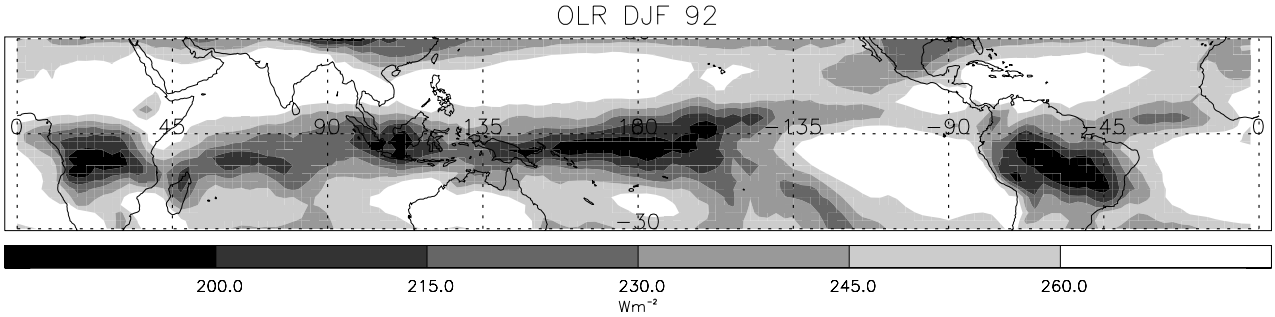

Figure 5. December–February averaged OLR from AVHRR. Low values indicate higher cloud tops.

They have passed though the convectively active regions and it may be that they are left over from previous convective events, as it has been noted [*Pfister et al.*, 2001] that convective outflow cirrus is not always dissipated rapidly and can remain in the tropopause region for extended periods of time.

3.1.2. Trajectories Ending at 83 hPa

[24] At 83 hPa (Figure 6) the relative contributions of each category of vertical motion to the total is different from that at 68 hPa, but the horizontal patterns of the trajectories remain similar to Figure 3. The "descent" category in most regions accounts for fewer trajectories at 83 hPa than at 68 hPa. The exceptions to this are over Africa and the Atlantic where the contribution from descending air has increased. This probably indicates that the inverse circulation found above convection noted by *Norton* [2001], begins closer to the 83 hPa level over Africa and the Atlantic and closer to 68 hPa in the Indonesian and Pacific ocean sectors.

[25] We see that the contribution from "zonal ascent" is smaller at 83 hPa than at 68 hPa but that the contribution from rapid ascent is much greater. Again, the greatest contribution from rapid ascent is in the central and western Pacific where deep convection is the most prevalent. If all the cirrus were to be found at 83 hPa we might infer that 68% of the cirrus formation over the central Pacific had some convective component and that the importance of this convective component lessens with increasing height as the importance of zonal ascent increases. This percentage is similar to that found by *Spang et al.* [2002] using data from the Cryogenic Infrared Spectrometers and Telescopes for the Atmosphere (CRISTA) instrument. They found that about 75% of cirrus at about 15 km in the 80°E to 300° in August 1997 stemmed from convective systems and inferred that around one quarter were the result of other mechanisms such as in situ cooling. The percentage contribution from rapid ascent is likely to change significantly with both geographical location and season, however. *Massie et al.* [2002] found that around half of cirrus observed from the HALOE instrument during 1995–2000 in the maritime continent were related to convective outflow. The eastward displacement that we observe in 1992 relative to the HALOE 1995–2000 climatology may be due to the El Niño conditions of 1992 which has been shown to displace cirrus clouds eastward along with an eastward shift in OLR [*Massie et al.*, 2000; *Gettelman et al.*, 2001].

3.2. Cirrus, Water Vapor, and Ozone

[26] Cirrus clouds may play an important role in accounting for the dryness of the lower stratosphere and for this reason, we examine the MLS water vapor field to see whether areas of saturation are well correlated with the location of cirrus. Similarly we examine the MLS ozone field, as ozone is a useful tracer for following atmospheric motions in the tropical tropopause region. Ozone mixing ratios increase sharply on ascending from the troposphere to the stratosphere and observations of air with low mixing ratio in the stratosphere can be used to indicate where air has had recent contact with the troposphere [e.g., *Randel et al.*, 2001].

[27] Again, we examine data at 68 hPa where we have observations of water vapor and ozone from MLS. First we calculate the relative humidity with respect to ice (RHi) for each cloud observation using the ECMWF temperature at the nearest grid point and the nearest synoptic time to the MLS measurement of water vapor mixing ratio. MLS and CLAES have similar viewing characteristics (see section 2) with the footprints lying close to each other. We discard any observations which are more than 50 km apart. The footprint size is about 25 km × 400 km and hence the footprints do not overlap and we must assume some coherence of the footprint averages of water vapor, ozone and temperature on a scale of a few hundred kilometers.

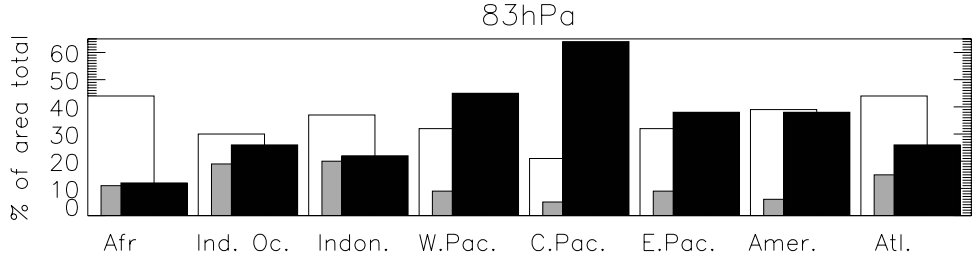

Figure 6. Same as for Figure 2 but assuming clouds to be at 83 hPa.

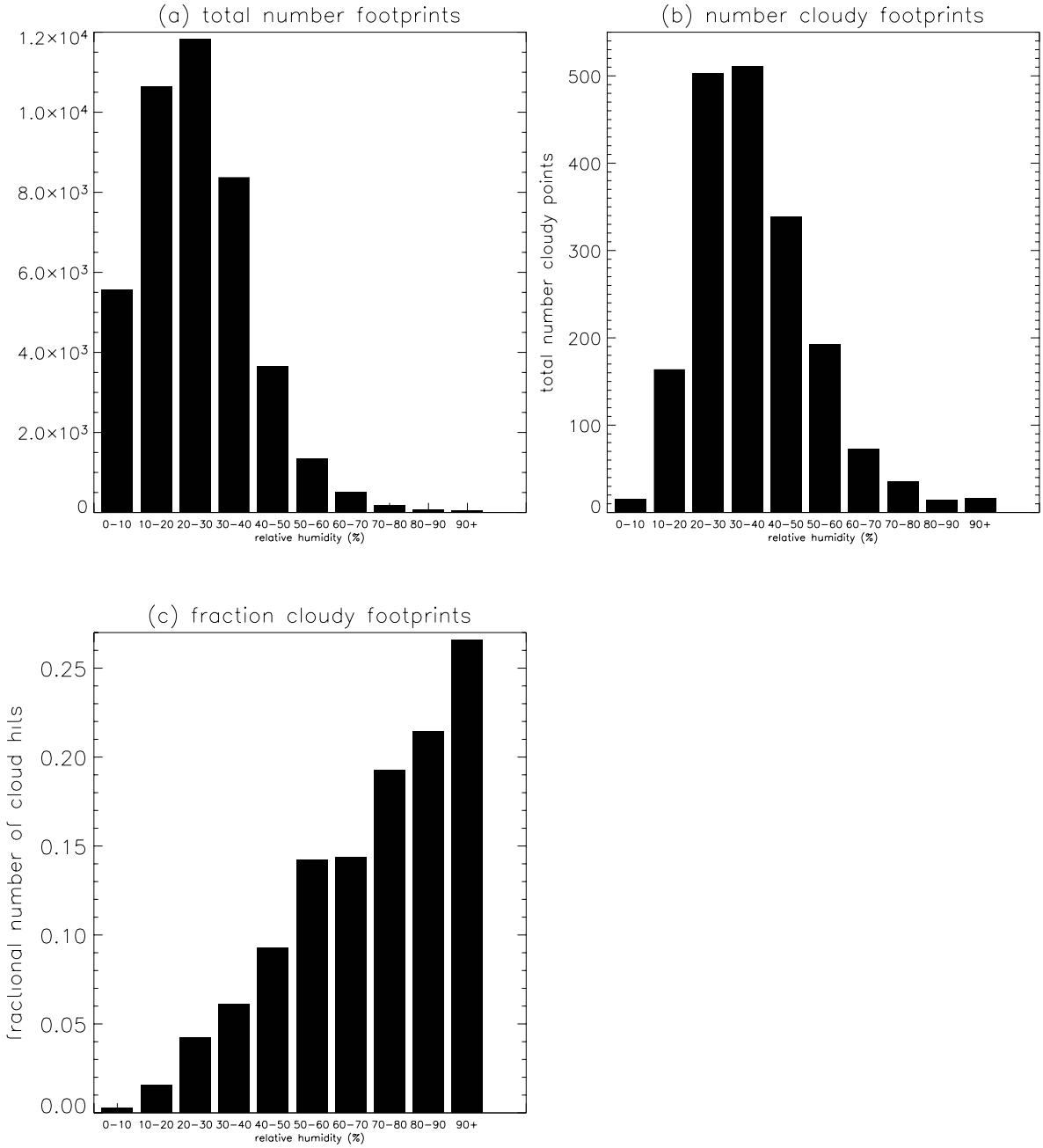

Figure 7. Histogram of the fraction of MLS footprints which contain a CLAES cloud for 10% relative humidity bins for December 1991 to February 1992 at 68 hPa.

[28] *Simmons et al.* [1999] reported that ECMWF temperatures at 90 hPa in boreal winter 1996/1997 were higher than minimum sonde temperatures by 2.5°C at Kota Kinabulu and 1.8°C at Truk (both stations in the tropics). He noted that the vertical resolution of the ECMWF model was only 20 hPa at the 90 hPa level and that the overestimation of temperature was to be expected, leading to an underestimation of the degree of drying of the air as it enters the stratosphere. At 68 hPa this temperature difference could change relative humidities by about 10%. The reanalysis temperatures used here were compared by *Pawson and Fiorino* [1998] with NCEP temperatures and they found the tropical mean temperatures to be lower than the corresponding operational analysis (as 1996/1997 mentioned above), colder than the NCEP analysis and closer in agreement with radiosonde observations.

[29] We created 10 bins for RHi in 10% intervals, with the final bin being for RHi of 90% and over, and counted the number of clouds in each bin. Figure 7a shows the distribution of RHi found at 68 hPa in DJF 1991/92. Values range from 0 to 90+% with most air having an RHi of 20 to 30%. In Figure 7 (right), the number of cloudy footprints in each bin is plotted. Clouds are found over the full range of the measured RHi values. Although we might expect to find clouds only when the RHi reaches 100%, if the cloud is smaller than the footprint size, the average RHi across the footprint might be less than 100%. We return to this point

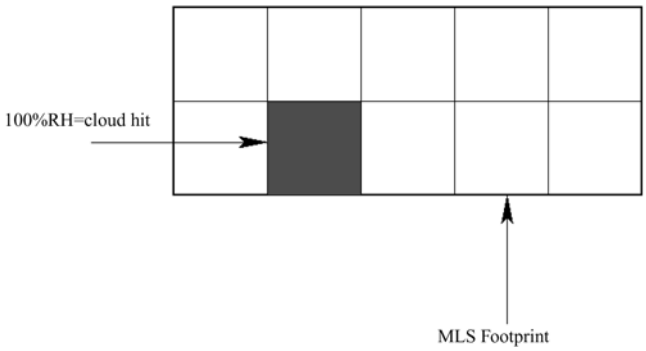

Figure 8. Representation of MLS footprint and the recording of the cirrus cloud.

later in this section. The distribution of clouds peaks at 30–40% and is shifted to the right compared with the distribution of RHi. We divide the number of clouds in each bin (Figure 7b) by the number of MLS footprints in each bin to give the fraction of the MLS footprints which contain a CLAES cloud. This is plotted in Figure 7c. Figure 7c thus shows that cirrus clouds are more likely to be found as the RHi increases. Clouds are more likely to be present in the regions where the air is more saturated, as we would expect, and as studies for the upper troposphere have shown. For example, *Sandor et al.* [2000] used MLS data and CLAES measurements at 147 hPa and found that cirrus frequency increased with relative humidity.

[30] As mentioned above, we might expect to find clouds only when the relative humidity hits 100% but in fact we see clouds in air with a range of relative humidities. We designed a simple model to illustrate how this can arise. The model represents how MLS would measure relative humidity compared with the recording of a cirrus observation which we assume to be on a smaller horizontal scale than that of the MLS footprint. Each water vapor measurement is essentially an average over a horizontal area of about 25 × 400 km^2 and 3 km in the vertical. In the upper troposphere at around 215 hPa, comparison of MLS measurements with Lidar measurements have shown that high humidities are often present in narrow laminae [*Newell et al.*, 1996] and the small-scale variations of high humidity will be averaged with lower humidity regions over the MLS footprint. Even in the lower stratosphere, 5-day averaged water vapor fields from MLS show that there is still considerable spatial variability [*Clark et al.*, 2001].

[31] Each footprint, represented by the large box in Figure 8, is divided into 10 smaller boxes. Each of the small boxes is assigned a random value for RHi ranging from 0 to 100% and based loosely on the observed mean and standard deviation as seen in Figure 7a. The division of the MLS footprint into 10 boxes is arbitrary, but tests show that the histograms are not very sensitive to the number of boxes in the footprint. If the RHi of any of the small boxes is 100%, then a cloud observation is recorded. The RHi of the large boxes or footprints is the average of all the smaller boxes. Figure 9 (left) shows the RHi of the footprints (unshaded), and the distribution of clouds within the RHi bins in grey. The distribution of the clouds within the RHi bins is again shifted to the right as the satellite data showed. Figure 9 (right) shows the probability of finding a cloud in each bin and this increases with RHi, again as the satellite results suggested. Thus the model illustrates that the results from the satellite are physically realistic. The distribution we obtain is as we would expect if the cirrus clouds are not filling the field of view of CLAES and if MLS does not record saturation because there is unsaturated air also in the footprint.

[32] Figure 10 shows the locations of saturated footprints at 68 hPa. Throughout the DJF period, there are few times that saturation is reached at this altitude but as the model

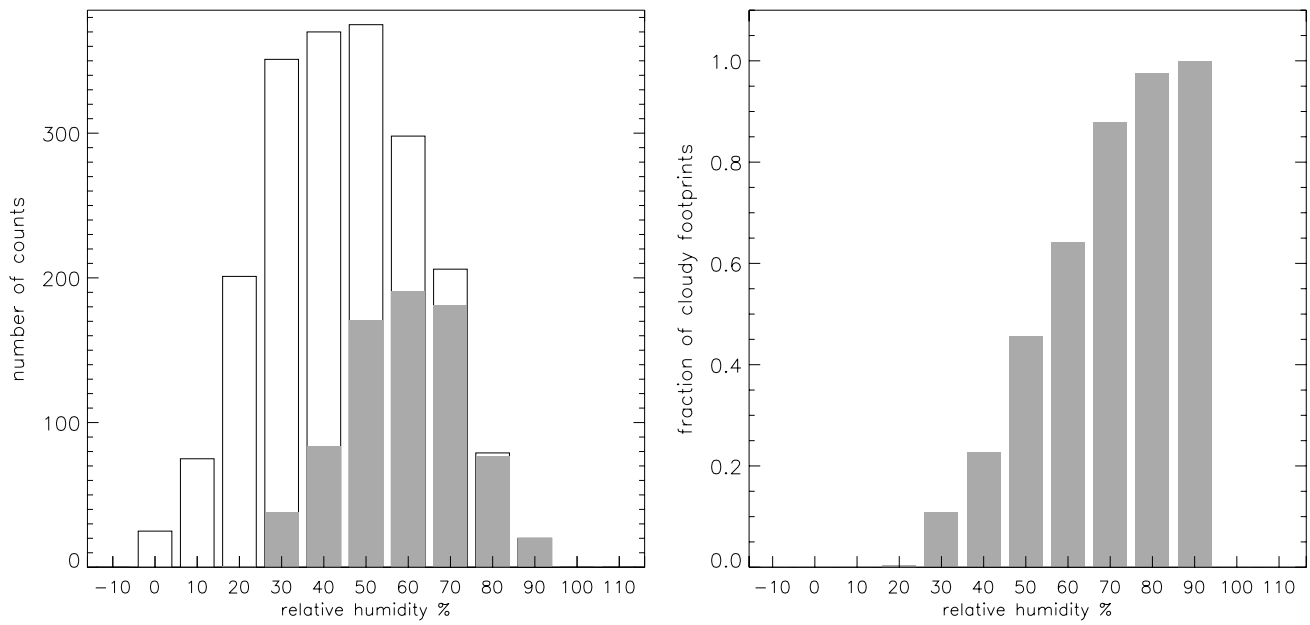

Figure 9. Model of cloud distributions based on relative humidity at 68 hPa. (left) Distribution of RH values of the footprints (unshaded) and the distribution of cloudy footprints shown in grey. (right) Probability of finding a cloud in a given RH bin.

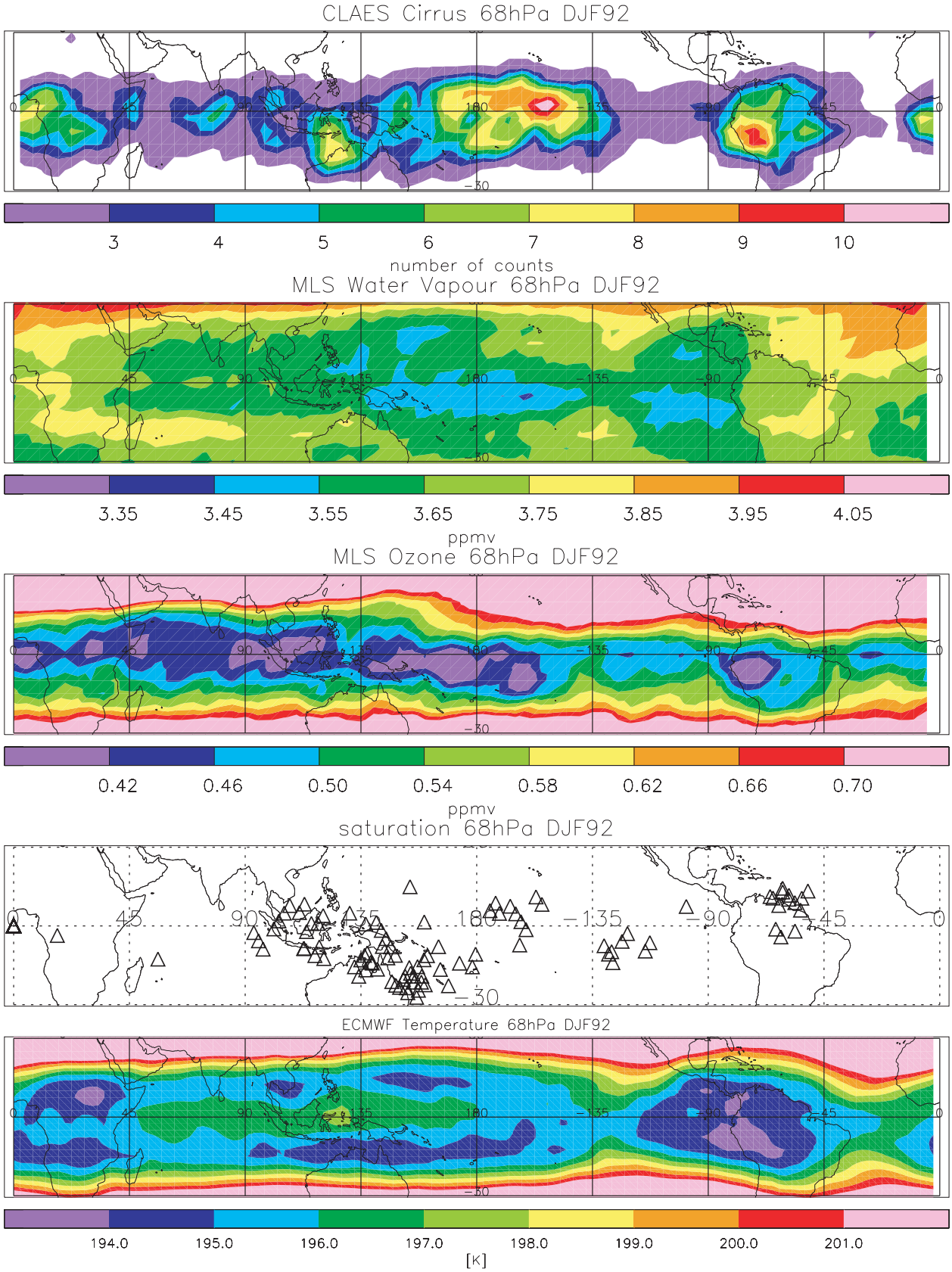

Figure 10. Seasonal averages of Cirrus frequency, water vapor mixing ratio, ozone mixing ratio, and collection of saturated footprints and ECMWF temperature for December–February 1991/1992.

and the bar charts illustrate, this is not necessarily because saturation is not occurring. The regions of saturation are found over the northeastern corner of Australia, a feature noted by *Kelly et al.* [1993], who showed that cloud edges in the tropopause region over northern Australia during the convectively active monsoon coincided with 100% ice saturation. There are also occasional incidences of saturation in the western Pacific, the region of the South Pacific Convergence Zone (SPCZ) and in South America.

[33] We repeat this analysis combining the CLAES cirrus with the ECMWF temperature field and the MLS ozone field. The histograms (not shown) indicate that cirrus are more likely in air with a temperature of between 188 to 190 K, the coldest temperatures being 186–188 K. There is some regional variation to this with the temperatures over Africa being a minimum of only 190–192 K and over South America of 188–190 K. Both Indonesia and the western Pacific have modal temperatures of 188–190 K but minimum values of 186–188 K.

[34] Similarly, we are more likely to find cirrus clouds in air of low ozone mixing ratios in a range of 0.1–0.2 ppmv. Such values of 100–200 ppbv or 0.1–0.2 ppmv are often used to differentiate between stratospheric and tropospheric air [*Danielsen*, 1968; *Shapiro*, 1980; *Pan et al.*, 1997]. The results may therefore suggest that air in which the cirrus are found has had more recent contact with the troposphere, but as *Roumeau et al.* [2000] showed, ozone can be destroyed on the surface of the ice in tropical cirrus clouds. The results are thus inconclusive that the air in which the cirrus are found has had recent contact with the troposphere and given that our trajectory analysis shows that air is not always ascending in cloudy regions, it is possible that some ozone destruction is taking place.

[35] In Figure 10 we see that the geographical location of the low water vapor mixing ratios, cirrus cloud cover and low ozone mixing ratios at 68 hPa tend to coincide well over the western Pacific. Likewise they correspond well to the location of low OLR values (Figure 5) indicating the areas of deep convection and ECMWF diabatic heating rates (Figure 4) indicating where motion is downward. *Randel et al.* [2001] found that lower in the tropical tropopause layer at around 100 hPa the water vapor minima are displaced in latitude with respect to the coldest temperatures and the deepest convection. Generally the water vapor minima are found in the Northern Hemisphere at this height [*Randel et al.*, 1998; *Pumphrey et al.*, 2000], the coldest temperatures roughly on the equator, and the deepest convection just south of the equator. By 68 hPa however, the water vapor minima are located more or less on the equator. Over south America, although the low ozone, cirrus and low temperatures all coincide geographically over Ecuador, saturation and negative diabatic heating are found further north and east over Venezuela and OLR is coldest over central Brazil. This misalignment over South America is similar to that shown by *Randel et al.* [2001] at 100 hPa and is in contrast to the western Pacific suggesting that mechanisms for dehydration in the two places may be different.

4. Conclusions

[36] In this paper we have described some of the characteristics of cirrus clouds observed by CLAES in the tropical tropopause region during northern hemisphere winter of 1991/1992, an El Niño period. The aim of the analysis was to see what the observations of cirrus can reveal about stratosphere-troposphere exchange and the movement of air within the tropical tropopause layer, and to see if cirrus can account for the low water vapor mixing ratios in the lower stratosphere. The trajectory analysis showed that there are a mixture of transport processes going on which are more or less important at different heights and geographical locations and at different times. The trajectory analysis also highlighted the importance of quasi-horizontal transport into the tropical region.

[37] At 68 hPa, a large fraction of cirrus (up to 50% over Africa), resulted from widespread zonal ascent. The trajectories traveled long distances in the horizontal over the 10 day period. They often originated in the extratropics, were carried by the westerly jets and turned toward the equator in subtropical anticyclones.

[38] In the Indonesian sector negative diabatic heating was observed which is suggestive of descending air. The trajectories showed that around 30% of cirrus formed in air which was descending. These results offer some support to the idea of *Sherwood* [2000] and *Gettelman et al.* [2000], who noted that air was often descending in the stratospheric "fountain" region. It is possible that these cirrus were formed in cooling descending air following a mechanism such as that proposed by *Hartmann et al.* [2001] and *Holton and Gettelman* [2001] in which cirrus that lie above deep convection produce radiative cooling and sinking and are sustained by horizontal transport of moister air into the cooler region.

[39] At 83 hPa, the percentage of cirrus with trajectories that have experienced an ascent more rapid than that which can be explained by the zonal mean uplift was larger than at 68 hPa. Most were found in the western Pacific and Indonesia where the majority of deep convection takes place. In these regions up to 60% of cirrus could have been influenced by convective processes, a figure which is similar to that of *Massie et al.* [2002]. This percentage contribution from convection to cirrus formation is highly dependent on season and on location.

[40] We found that the number of cirrus clouds increased as the relative humidity increased but that clouds can be found in air of very low footprint-averaged relative humidity. Ozone mixing ratios tended to be lower in the areas where cirrus were found. This could be due to the air having had more recent contact with the troposphere, an observation that would offer some insights into transport and the role of convection in the tropical tropopause layer. The other possibility is that ozone could be destroyed on the surface of the ice crystals in tropical cirrus clouds. Given that our trajectory analysis showed that air was not always ascending in cloudy regions, it is possible that some ozone destruction was taking place. Unfortunately, the UARS measurements of other chemical tracers in the lower stratosphere are not sufficiently well known to help distinguish between these possibilities. The new Earth Observing System Microwave Limb Sounder will provide measurements of such chemical species and should be able to do so in the presence of cirrus. We look forward to the launch of EOS MLS to enable us to clarify these issues.

[41] **Acknowledgments.** This work was funded by NERC in the United Kingdom and by CNRS in France.

References

Barath, F., et al., The Upper Atmosphere Research Satellite Microwave Limb Sounder Instrument, *J. Geophys. Res.*, *98*, 10,751–10,762, 1993.

Boehm, M. T., and J. Verlinde, Stratospheric influence on upper tropospheric tropical cirrus, *Geophys. Res. Lett.*, *27*, 3209–3212, 2000.

Brewer, A. M., Evidence for a world circulation provided by the measurements of helium and water vapor distribution in the stratosphere, *Q. J. R. Meteorol. Soc.*, *75*, 351–363, 1949.

Clark, H. L., A. Billingham, R. S. Harwood, and H. C. Pumphrey, Water vapor in the tropical lower stratosphere during the driest phase of the atmospheric tape recorder, *J. Geophys. Res.*, *106*, 22,695–22,705, 2001.

Danielsen, E. F., Stratospheric-tropospheric exchange based upon radioactivity, ozone and potential vorticity, *J. Atmos. Sci.*, *25*, 502–518, 1968.

Danielsen, E. F., A dehydration mechanism for the stratosphere, *Geophys. Res. Lett.*, *9*, 605–608, 1982.

Danielsen, E. F., In situ evidence of rapid, vertical, irreversible transport of lower tropospheric air into the lower tropical stratosphere by convective cloud turrets and by larger-scale upwelling in tropical cyclones, *J. Geophys. Res.*, *98*, 8665–8681, 1993.

Dessler, A. E., A reexamination of the "stratospheric fountain" hypothesis, *Geophys. Res. Lett.*, *22*, 4165–4168, 1998.

Dessler, A. E., Reply to comment by H. Vömel and S. J. Oltmans on "A reexamination of the 'stratospheric fountain' hypothesis," *Geophys. Res. Lett.*, *26*, 2739, 1999.

Dickenson, R. E., On the excitation of and propagation of zonal winds in an atmosphere with Newtonian cooling, *J. Atmos. Sci.*, *25*, 269–279, 1968.

Eliassen, A., Slow thermally or frictionally controlled meridional circulation in a circular vortex, *Astrophys. Norv.*, *5*(2), 19–60, 1951.

Froidevaux, L., et al., Validation of UARS Microwave Limb Sounder ozone measurements, *J. Geophys. Res.*, *101*, 10,017–10,060, 1996.

Gettelman, A., and P. M. de F. Forster, A climatology of the tropical tropopause layer, *J. Meteorol. Soc. Jpn.*, *80*, 911–924, 2002.

Gettelman, A., J. R. Holton, and A. R. Douglass, Simulations of water vapor in the lower stratosphere and upper troposphere, *J. Geophys. Res.*, *105*, 9003–9023, 2000.

Gettelman, A., W. J. Randel, S. Massie, F. Wu, W. G. Read, and J. M. Russell III, El-Niño as a natural experiment for studying the tropical tropopause region, *J. Clim.*, *14*, 3375–3392, 2001.

Gettelman, A., W. J. Randel, F. Wu, and S. T. Massie, Transport of water vapor in the tropical tropopause layer, *Geophys. Res. Lett.*, *29*(1), 1009, doi:10.1029/2001GL013818, 2002.

Gibson, J. K., P. Kallberg, S. Uppala, A. Hernandez, A. Nomura, and E. Serrano, ERA description, *ECMWF Re-anal. Proj. Rep. Ser. 1*, Eur. Cent. for Medium-Range Weather Forecasts, Reading, U. K., 1997.

Hartmann, D. L., J. R. Holton, and Q. Fu, The heat balance of the tropical tropopause cirrus and stratospheric dehydration, *Geophys Res. Lett.*, *28*, 1969–1973, 2001.

Holton, J. R., and A. Gettelman, Horizontal transport and the dehydration of the stratosphere, *Geophys Res. Lett.*, *28*, 2799–2802, 2001.

Jackson, D. R., J. Methven, and V. D. Pope, Transport in the low-latitude tropopause zone diagnosed using particle trajectories, *J. Atmos. Sci.*, *58*, 173–192, 2001.

Jensen, E. J., O. B. Toon, L. Pfister, and H. B. Selkirk, Dehydration of the upper troposphere and lower stratosphere by subvisible cirrus clouds near the tropical tropopause, *Geophys. Res. Lett.*, *23*, 825–828, 1996.

Jensen, E. J., W. G. Read, J. Mergenthaler, B. J. Sandor, L. Pfister, and A. Tabazadeh, High humidities and subvisible cirrus near the tropical tropopause, *Geophys. Res. Lett.*, *26*, 2347–2350, 1999.

Kelly, K. K., M. H. Proffitt, K. R. Chan, M. Loewenstein, J. R. Podolske, S. E. Strahan, J. C. Wilson, and D. Kley, Water vapor and cloud water measurements over Darwin during the STEP 1987 tropical mission, *J. Geophys. Res.*, *98*, 8713–8724, 1993.

Kent, G. S., E. R. Williams, P. H. Wang, M. P. McCormick, and K. M. Skeens, Surface temperature related variations in tropical cirrus cloud as measured by SAGE II, *J. Clim.*, *8*, 2577–2594, 1995.

Liebmann, B., and C. A. Smith, Description of a complete (interpolated) outgoing longwave radiation dataset, *Bull. Am. Meteorol. Soc.*, *77*, 1275–1277, 1996.

Liou, K.-N., Influence of cirrus clouds on weather and climate processes: A global perspective, *Mon. Weather Rev.*, *114*, 1167–1199, 1986.

Livesey, N. J., W. G. Read, L. Froidevaux, J. W. Waters, H. C. Pumphrey, D. L. Wu, M. L. Santee, Z. Shippony, and R. F. Jarnot, The UARS Microwave Limb Sounder version 5 data set; Theory, characterization, and validation, *J. Geophys. Res.*, *108*(D13), 4378, doi:10.1029/2002JD002273, 2003.

Luo, Z., W. B. Rossow, T. Inoue, and C. J. Stubenrauch, Did the eruption of Mt. Pinatubo affect cirrus properties?, *J. Clim.*, *15*, 2806–2820, 2002.

Massie, S. T., P. Lowe, X. Tie, M. Hervig, G. Thomas, and J. Russell III, Effect of the 1997 El Niño on the distribution of upper tropospheric cirrus, *J. Geophys. Res.*, *105*, 22,725–22,741, 2000.

Massie, S., A. Gettelman, W. Randel, and D. Baumgardner, Distribution of tropical cirrus in relation to convection, *J. Geophys. Res.*, *107*(D21), 4591, doi:10.1029/2001JD001293, 2002.

Mergenthaler, J. L., A. E. Roche, J. B. Kumer, and G. A. Ely, Cryogenic Limb Array Etalon Spectrometer observations of tropical cirrus, *J. Geophys. Res.*, *104*, 22,183–22,194, 1999.

Methven, J., Offline trajectories: Calculation and accuracy, *UGAMP Tech. Rep. 44*, UK Univ. Global Atmos. Modell. Programme, Reading, U.K., 1997.

Michelsen, H. A., F. W. Irion, G. L. Manney, G. C. Toon, and M. R. Gunson, Features and trends in Atmospheric Trace Molecule Spectroscopy (ATMOS) version 3 stratospheric water vapor and methane measurements, *J. Geophys. Res.*, *105*, 22,713–22,724, 2000.

Mote, P. W., K. H. Rosenlof, J. S. Holton, R. S. Harwood, and J. W. Waters, Seasonal variations of water vapour in the tropical lower stratosphere, *Geophys. Res. Lett.*, *22*, 1093–1096, 1995.

Mote, P. W., K. H. Rosenlof, M. E. McIntyre, E. S. Carr, J. C. Gille, J. S. Holton, J. S. Kinnersley, H. C. Pumphrey, J. M. Russell III, and J. W. Waters, An atmospheric tape recorder: The imprint of tropical tropopause temperatures on stratospheric water vapour, *J. Geophys. Res.*, *101*, 3989–4006, 1996.

Newell, R. E., and S. Gould-Stewart, A stratospheric fountain?, *J. Atmos. Sci.*, *38*, 2789–2796, 1981.

Newell, R. E., Y. Zhu, E. V. Browell, S. Ismail, W. G. Read, J. W. Waters, K. K. Kelly, and S. C. Liu, Upper tropospheric water vapour and cirrus: Comparison of DC-8 observations, preliminary UARS microwave-limb sounder measurements and meteorological analyses, *J. Geophys. Res.*, *101*, 1931–1941, 1996.

Norton, W. A., Longwave heating of the tropical lower stratosphere, *Geophys. Res. Lett.*, *28*, 3653–3656, 2001.

Pan, L., S. Solomon, W. Randel, J.-F. Lamarque, P. Hess, J. Gille, E.-W. Chiou, and M. P. McCormick, Hemispheric asymmetries and seasonal variations of the lowermost water vapor and ozone derived from SAGE II data, *J. Geophys. Res.*, *102*, 28,177–28,184, 1997.

Pawson, S., and M. Fiorino, A comparison of reanalyses in the tropical stratosphere. part 1: Thermal structure and the annual cycle, *Clim. Dyn.*, *14*, 631–644, 1998.

Pfister, L., et al., Aircraft observations of thin cirrus clouds near the tropical tropopause, *J. Geophys. Res.*, *106*, 9765–9786, 2001.

Potter, B. E., and F. R. Holton, The role of monsoon convection in the dehydration of the lower tropical stratosphere, *J. Atmos. Sci.*, *52*, 1034–1050, 1995.

Pumphrey, H. C., Validation of a new prototype water vapor retrieval for UARS MLS, *J. Geophys. Res.*, *104*, 9399–9412, 1999.

Pumphrey, H. C., H. L. Clark, and R. S. Harwood, Lower stratospheric water vapour measured by UARS MLS, *Geophys. Res. Lett.*, *27*, 1691–1694, 2000.

Ramanathan, V., and W. Collins, Thermodynamic regulation of ocean warming by cirrus clouds deduced from observations of the 1987 El Niño, *Nature*, *349*, 500–503, 1991.

Randel, W. J., F. Wu, J. M. Russell III, A. Roche, and J. W. Waters, Seasonal cycles and QBO variations in stratospheric CH_4 and H_2O observed in UARS HALOE data, *J. Atmos. Sci.*, *55*, 163–185, 1998.

Randel, W. J., F. Wu, A. Gettelman, J. M. Russell III, J. M. Zawodny, and S. J. Oltmans, Seasonal variation of water vapor in the lower stratosphere observed in Halogen Occultation Experiment data, *J. Geophys. Res.*, *106*, 14,313–14,325, 2001.

Read, W. G., et al., UARS MLS upper tropospheric humidity measurement: Method and validation, *J. Geophys. Res.*, *106*, 32,207–32,258, 2001.

Reber, C. A., The Upper Atmosphere Research Satellite (UARS), *Geophys. Res. Lett.*, *20*, 1215–1218, 1993.

Robinson, G. D., The transport of minor atmospheric constituents between the troposphere and stratosphere, *Q. J. R. Meteorol. Soc.*, *106*, 227, 1980.

Roche, A. E., J. B. Kumer, J. L. Mergenthaler, G. A. Ely, W. G. Uplinger, J. F. Potter, T. C. James, and L. W. Sterritt, The Cryogenic Limb Array Etalon Spectrometer (CLAES) on UARS: Experiment description and performance, *J. Geophys. Res.*, *98*, 10,763–10,775, 1993.

Roumeau, S., P. Brémaud, E. Rivière, S. Baldy, and J. L. Baray, Tropical cirrus clouds: A possible sink for ozone, *Geophys. Res. Lett.*, *27*, 2233–2236, 2000.

Sandor, B., E. Jensen, E. Stone, W. Read, J. Waters, and J. Mergenthaler, Upper Tropospheric Humidity and Thin Cirrus, *Geophys. Res. Lett.*, *27*, 2645–2648, 2000.

Sassen, K., and B. S. Cho, Subvisual-thin cirrus clouds lidar dataset for satellite verification and climatological research, *J. Appl. Meteorol. Soc.*, *31*, 1275–1285, 1992.

Shapiro, M. A., Turbulent mixing within tropopause folds as a mechanism for the exchange of chemical constituents between the stratosphere and the troposphere, *J. Atmos. Sci.*, *37*, 994–1004, 1980.

Sherwood, S. C., A "stratospheric drain" over the maritime continent, *Geophys. Res. Lett.*, *27*, 677–680, 2000.

Sherwood, S. C., and A. E. Dessler, On the control of stratospheric humidity, *Geophys. Res. Lett.*, *27*, 2513–2516, 2000.

Simmons, A. J., A. Untch, C. Jakob, P. Kallberg, and P. Unden, Stratospheric water vapour and the tropical tropopause temperatures in ECMWF analyses and multi-year simulations, *Q. J. R. Meteorol. Soc*, *25*, 353–386, 1999.

Spang, R., G. Eidmann, M. Riese, D. Offermann, P. Preusse, L. Pfister, and P.-H. Wang, CRISTA observations of cirrus clouds around the tropopause, *J. Geophys. Res.*, *107*(D23), 8174, doi:10.1029/2001JD000698, 2002.

Vömel, H., and S. J. Oltmans, Comment on "A reexamination of the 'stratospheric fountain' hypothesis" by A. E. Dessler, *Geophys. Res. Lett.*, *26*, 2737–2738, 1999.

Wang, P.-H., P. Minnis, M. P. McCormick, G. S. Kent, and K. M. Skeens, A 6-year climatology of cloud occurrence frequency from Stratospheric Aerosol and Gas Experiment II observations (1985–1990), *J. Geophys. Res.*, *101*, 29,407–29,429, 1996.

Waters, J. W., Microwave Limb Sounding, in *Atmospheric Remote Sensing by Microwave Radiometry*, edited by M. A. Janssen, pp. 383–496, John Wiley, Hoboken, N. J., 1993.

Winker, D. M., and C. R. Trepte, Laminar cirrus observed near the tropical tropopause by LITE, *Geophys Res. Lett.*, *25*, 3351–3354, 1998.

Zhou, X.-L., M. A. Geller, and M. Zhang, Cooling trend of the tropical cold point tropopause temperatures and its implications, *J. Geophys. Res.*, *106*, 1511–1522, 2001.

A. Billingham, R. S. Harwood, and H. C. Pumphrey, School of GeoSciences, University of Edinburgh, West Mains Road, Edinburgh EH9 3JZ, UK. (aaron@met.ed.ac.uk; r.s.harwood@ed.ac.uk; hcp@met.ed.ac.uk)

H. L. Clark, Centre National de Recherches Météorologiques, 42 Ave. Gaspard Coriolis, F-31057 Toulouse Cedex 1, France. (hannah.clark@cnrm.meteo.fr)